ENERGY EFFICIENT BELT CONVEYOR DESIGN

Craig Wheeler, Paul Munzenberger, Daniel Ausling and Brendan Beh

TUNRA Bulk Solids Research Associates
The University of Newcastle, Australia

ABSTRACT

The University of Newcastle has undertaken a systematic research program to identify, model and measure key design elements to reduce the energy consumption of belt conveyors. Research outcomes include the development of theoretical models to accurately predict the main resistances of belt conveyors, in parallel with developing extensive test facilities to verify the new models and to provide industry with data that can be used directly in the design process.

This paper discusses the application of these models and test results for conveyor design, demonstrating the advantages of informed component selection to not only reduce energy consumption, but also total cost of ownership. In particular, the combination of design parameters is discussed in relation to the rotating resistance of idler rollers, conveyor belt indentation rolling resistance and conveyor belt and bulk material flexure resistance. Through a combination of theoretical models and measured data, trends are identified to assist in the design of energy efficient belt conveyor systems.

1. INTRODUCTION

Ideally, the design of a belt conveyor system incorporates a combination of design parameters that minimise energy consumption and lifecycle cost. Too often, conveyor design is driven to minimise capital cost, rather than considering the total cost of ownership. Informed component selection at the design stage can often lead to both a cost effective and energy efficient solution. This paper aims to identify key design parameters for energy efficient conveyor design and assist designers develop more cost effective solutions.

Several authors have investigated the motion resistances of belt conveyors[1-6] while others have specifically investigated methods to minimise energy consumption[7,8,9]. The latter work identified key areas to minimise energy usage with indentation rolling resistance being a major area of interest due to its significant contribution to the overall resistance to motion. Increasing idler roller diameter, specialised belt constructions and low rolling resistance pulley covers were discussed[7]. Furthermore, the energy and cost benefits of increasing idler spacing are well documented[8,9].

While much research has been published on the topic, this paper hopes to add to the literature by demonstrating how data from laboratory tests (covered by a range of standards and handbook methods) can be used effectively in the design process. The approach adopted is to investigate the individual components of the motion resistance, present analytical models to predict each component and, in combination with laboratory test results, demonstrate its application for energy saving conveyor design.

Throughout the paper a number of testing standards and handbook methods are discussed in relation to motion resistance measurement. In some cases, the data obtained from these methods are able to be used directly for conveyor design. However, others only offer a means to compare, and are often not usable directly in the design process, since test parameters are typically different to system specifications. In some cases the results can be modified for design purposes, but must be done so with careful consideration of the fundamental relationships. This paper intends to draw the reader's attention to these underlying relationships and provide guidance in the application of test data to the design process.

2. BACKGROUND

During the design of a belt conveyor system, the demand power, take-up tension, and resulting steady state belt tension distribution is calculated for a range of loading conditions. Derivation of the various resistance components varies according to the standard or design method followed, while the slope resistances generally follow the same procedure. For the purpose of this paper, a straight horizontal belt conveyor is assumed, as shown in Figure 1.

Figure 1 outlines the components of motion resistance for a horizontal belt conveyor. The resistance components are notably different to those in DIN22101[10] and ISO5048[11] but similar to those referenced in CEMA[12]. The resistance components take into consideration individual contributions, rather than adding multiple resistances together. The motion resistance components include indentation rolling resistance, belt flexure resistance, idler roller rotating resistance, idler roller misalignment resistance and bulk material flexure resistance. Like DIN and ISO standards, the cumulative resistance along the length of the belt conveyor is calculated by superimposing the contributions from each of the motion resistances, as shown in Figure 1. Secondary resistance can also be included as a length coefficient based on the approach detailed in DIN or ISO.

With reference to Figure 1, the belt and bulk material flexure resistance components are shown (due to scaling) to linearly increase with length and therefore independent of tension. In practice, these components do in fact decrease per unit length, as belt tension increases. All other resistance components are considered to be independent of belt tension in the absence of any vertical and horizontal curves.

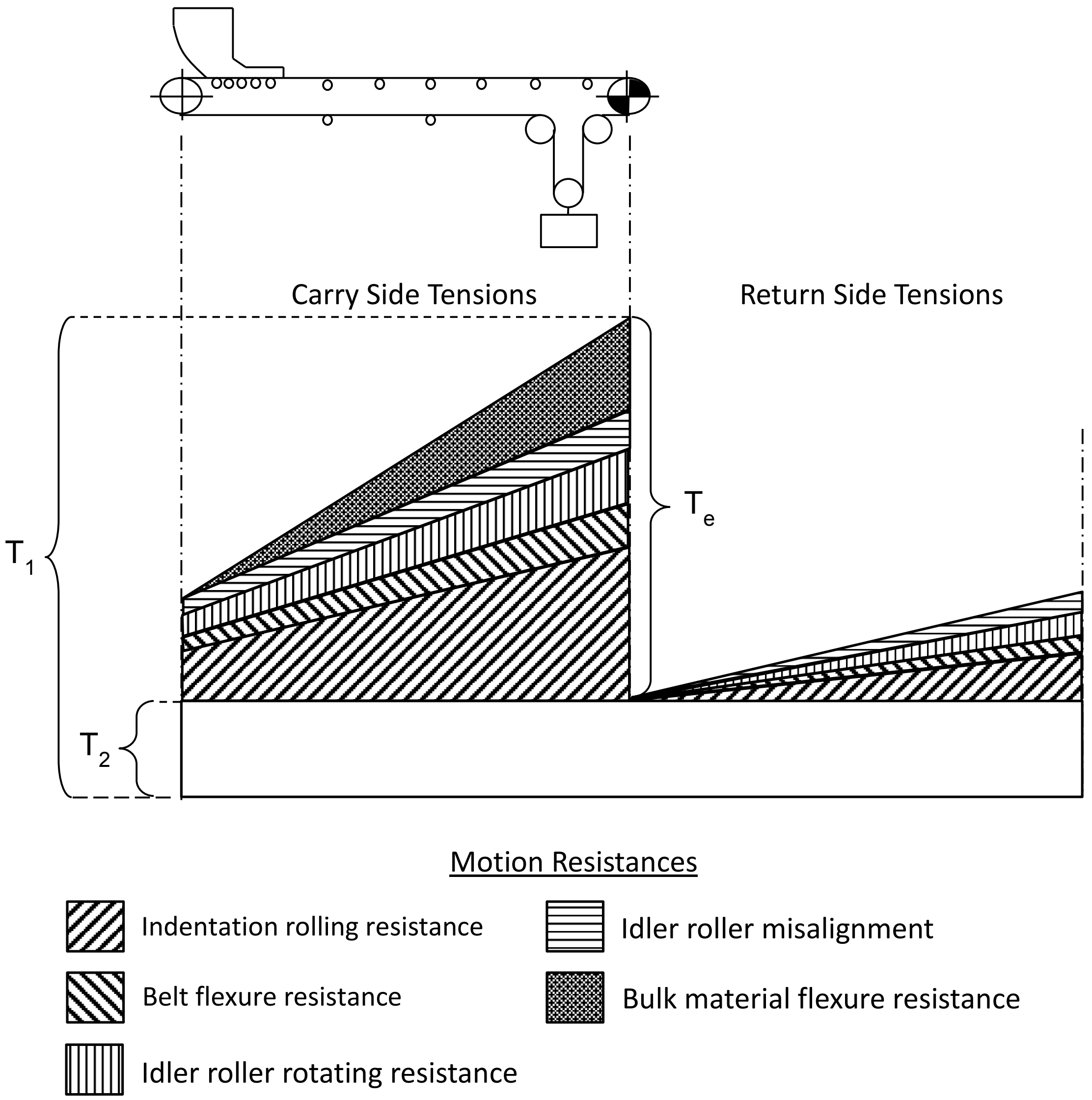

Figure 1. Steady state belt tension distribution for a horizontal belt conveyor

Each of the main resistance components are discussed in detail, analytical models are presented and, in combination with laboratory test data, trends identified to reduce the motion resistance. For the purpose of this paper the idler roller misalignment resistance will not be discussed, with the reader referred to CEMA[12] for a comprehensive treatment of this component.

3. IDLER ROLLER ROTATING RESISTANCE

The primary function of idler rollers in a belt conveyor system is to support the conveyor belt along its length. Predicting the cumulative resistance of idler rollers is vitally important in calculating the belt tension and therefore power requirements of a system, particularly on long overland conveyors where there are typically more than one thousand idler rollers per kilometre of belt.

The rotating resistance of idler rollers in belt conveyor systems occurs due to the friction of the rolling elements in the bearings, the viscous drag of the lubricant and the friction of the contact lip seals. The resistance force typically contributes between 5% to 15% [6,7] of the motion resistance of long horizontal belt conveyors. While this may be considered a relatively small contribution, when considering belt conveyor systems many kilometres in length, accurately determining this resistance is vital for the appropriate selection of drives and belting.

The rotating resistance of the idler rollers is primarily dependent on the seal type and configuration, the type of bearings, the temperature of the lubricant and the rotational speed of the idler roller. Contact lip seals and grease-filled labyrinth seals typically form the boundary preventing dust and water ingress into the rolling elements of the bearings. The labyrinth seals can be fully packed with grease to optimise the sealing efficiency of the labyrinth, resulting in viscous drag generated from the shearing of the grease between the layers of rotating and stationary surfaces. An outer contact lip seal typically forms the primary boundary between external contaminants entering the labyrinth seal, while an inner lip seal contains the lubricating grease within the bearing. The outer and inner contact lip seals add to the rotating resistance of the idler roller due to the nature of the sealing mechanism. In addition to the resistances associated with sealing, conventional idler rollers use rolling element bearings where the friction primarily depends on the bearing type and size, the operating speed, the properties and quantity of the lubricant and, to a lesser extent in the case of idler rollers, the load. The total resistance to rotation of a bearing is made up of the rolling and sliding friction between the rolling elements and the cage and guiding surface, and the internal friction of the lubricant[15].

EXPERIMENTAL MEASUREMENT

Several standards exist to measure the rotating resistance of idler rollers[13,14] with the measurement methods recommended in these standards being similar. The SANS method uses a rotating disc positioned directly above the idler roller that in turn drives the roller at 750 rpm and applies a 250 N vertical load at a temperature of 20^{o}C. The shaft of the idler roller is supported on a pivot which is restricted from rotating by a lever arm. Rotating resistance is calculated from the moment determined from the length of the lever and the force acting at the end of the lever arm. Figure 2 shows the total rotating resistance and bearing temperature for a $\varnothing$152 mm idler roller operating at 6 m/s at ambient temperatures of 20^{o}C and 0^{o}C. Both results clearly demonstrate the reduction in rotating resistance with running time, as the temperature of the grease within the bearings and the labyrinth seals increase.

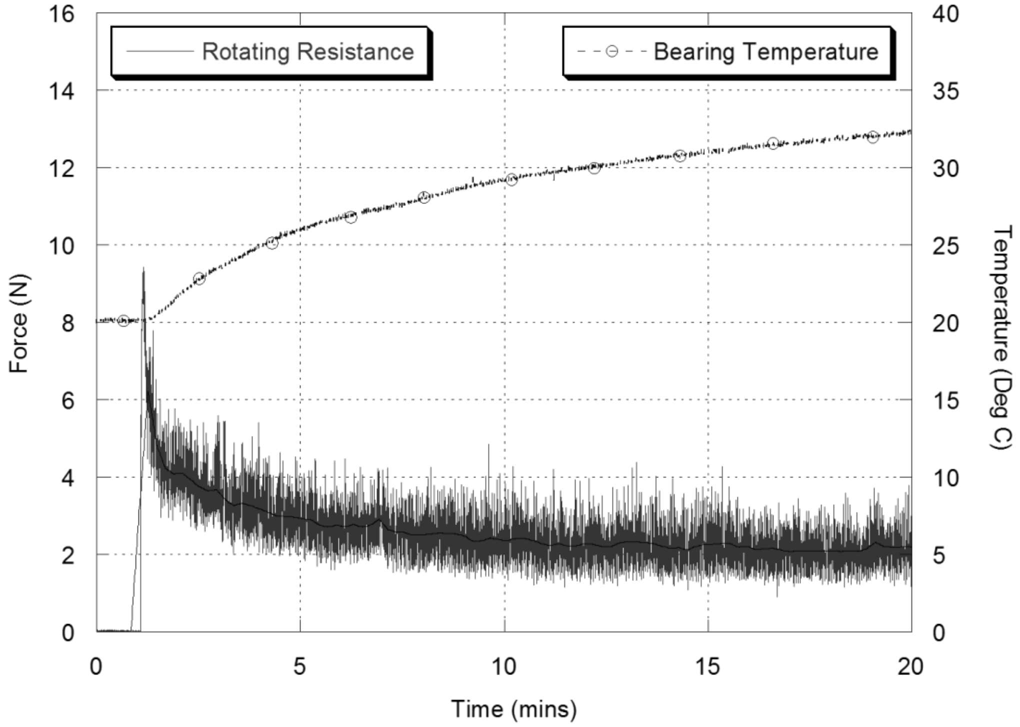

(a) 20°C ambient temperature

(b) 0°C ambient temperature

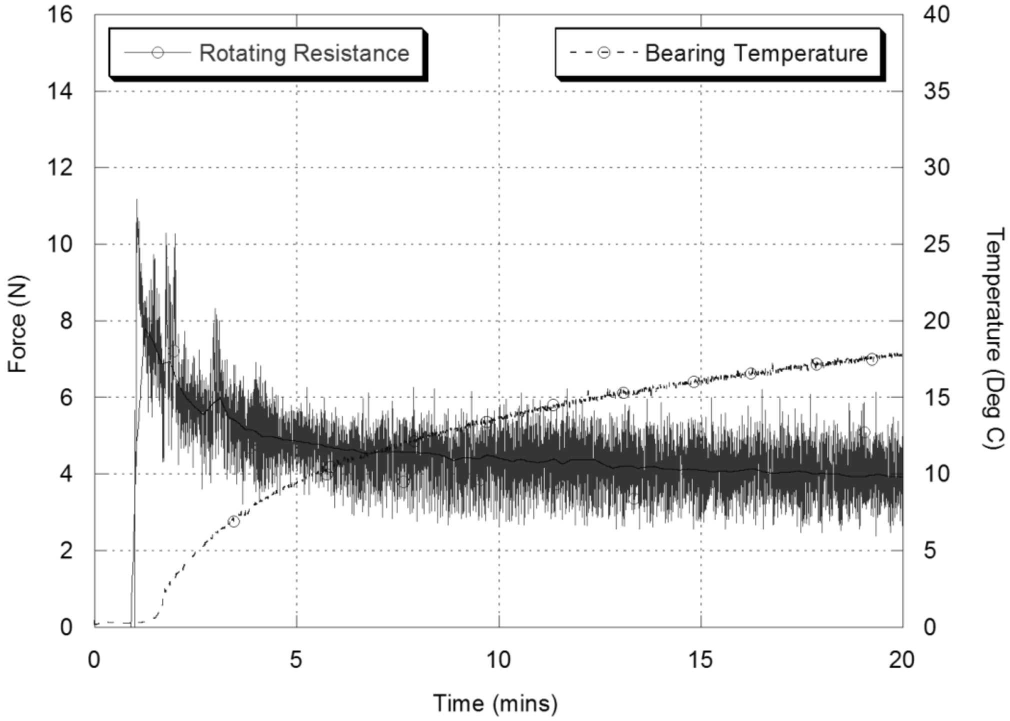

Figure 2. Idler roller rotating resistance and bearing temperature versus time for a Ø152 mm at 6 m/s

THEORETICAL PREDICTION

In order to theoretically predict the rotating resistance of idler rollers, each component that contributes to the resistance is calculated individually. The major components of the rotating resistance that are analysed include the viscous drag due to the shearing of the grease within the labyrinth seal F_{lab}, the friction of the rolling element bearings generated from the no-load and load dependent components F_{brg}, and the rotating resistance of the contact lip seals F_{ls}.

Labyrinth Seal Viscous Drag

Labyrinth seals consist of a stationary section fitted to the shaft of the idler roller and a rotating part housed into the idler shell. Due to the nature of the sealing mechanism, viscous drag is generated as a result of the shearing of the grease between the layers of rotating and stationary surfaces. The magnitude of the retarding moment depends on the viscosity of the lubricating grease, the rotational speed of the idler roller and physical configuration of the labyrinth seal.

The axial sealing arrangement shown schematically in Figure 3 may be simplified for analysis by ignoring the end effects of the discs and considering the arrangement as a number of concentric cylinders. In each layer of the labyrinth there is one stationary surface fixed to the shaft and one rotating surface attached to the shell of the idler roller. Figure 3 also shows schematically the simplified analysis and details the force balance at the interface between the seal and grease.

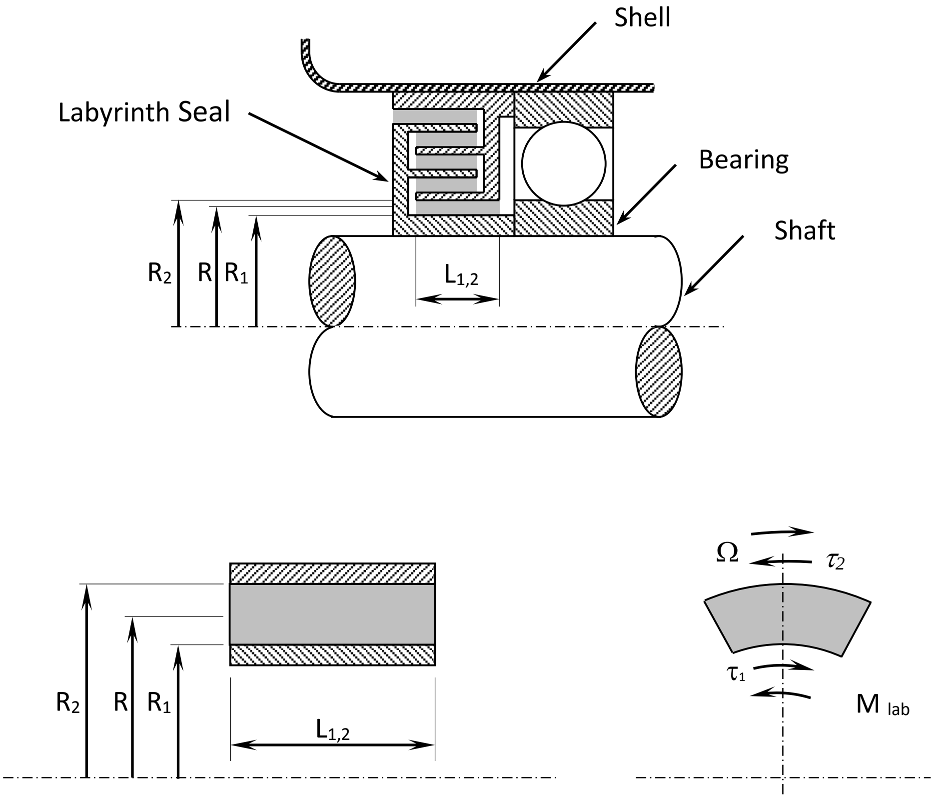

Figure 3. Typical labyrinth seal configuration and resistance analysis Wheeler[6].

M_{lab} is the moment acting due to the viscous drag of the labyrinth seal, Ω is the angular velocity of the idler roller and τ is the shear stress acting on an element of grease. The subscripts represent the concentric surfaces labelled from the centre outwards.

Grease may be considered a Newtonian fluid under normal operating conditions, with the force momentum balance for one-dimensional planar flow given by

$$\tau_{yx} = \mu \frac{du}{dy} \qquad 1$$

The shear stress τ_{yx} acting on the fluid element is subjected to a shear rate du/dy, where u is the velocity of the grease and y the position. The constant of proportionality is the absolute, or dynamic viscosity, μ. Provided the dynamic viscosity of the lubricating grease is constant throughout the labyrinth seal, the total moment acting due to the viscous drag is

$$M_{lab} = 4\pi\mu\Omega \left\{ \frac{L_{1,2}R_1^2}{\left[1-\left(\frac{R_1}{R_2}\right)^2\right]} + \frac{L_{3,4}R_3^2}{\left[1-\left(\frac{R_3}{R_4}\right)^2\right]} + \ldots\ldots.. + \frac{L_{2n-1,2n}R_{2n-1}^2}{\left[1-\left(\frac{R_{2n-1}}{R_{2n}}\right)^2\right]} \right\} \qquad 2$$

Where n is the number of concentric labyrinth surfaces. The resistance force per idler roller acting as a result of the resistance of the labyrinth seals is then given by

$$F_{lab} = \frac{4M_{lab}}{D} \qquad 3$$

where D is the diameter of the idler roller.

Ball and Roller Bearing Friction

Bearing friction in ball and roller bearings is generated due to the hysteresis formed within the contact zone. Conveyor idler roller bearings are generally grease lubricated due to the relatively low operating speeds and the ability to pre-pack the bearings for extended service life. The grease lubricant acts as a load transmitting element that prevents metal-to-metal contact between the rolling elements and, as such, the rolling elements experience a combination of hydrodynamic and boundary lubrication. The total friction moment for a bearing within an idler roller is determined from the sum of the no-load and load dependent moments. The frictional losses associated with grease lubricated bearings under no-load conditions are difficult to predict accurately, however an approximation of the no-load friction moment M_0 is given by Palmgren[15] as

$$M_0 = f_0 \times 10^{-1} (\nu s)^{2/3} d_m^3 \qquad 4$$

Provided

$$\nu s \geq 2000 \qquad 5$$

Where ν is the kinematic viscosity of the grease, s is the speed of rotation of the bearing and the relationship between the dynamic viscosity μ, and the kinematic viscosity ν, is

$$\mu = \nu\rho \qquad 6$$

where ρ is the density of the grease. The kinematic viscosity is also known as the base oil viscosity and is normally expressed in cSt, where 1cSt = 1×10^{-6} m^2/s. Additionally, d_m is the mean diameter of the bearing given by

$$d_m = 0.5(d_i + d_o) \qquad 7$$

where d_i is the inside diameter of the bearing and d_o is the outside diameter of the bearing. Furthermore f_0 in Equation 4 is a factor depending on the bearing design and lubrication method, where f_0 = 1.5 to 2.0 for single row deep groove ball bearings.

A load dependent friction moment M_1, due to the sliding resistance and hysteresis resistance of the bearing elements, is given by Palmgren[15] as

$$M_1 = f_1 F_r d_m \qquad 8$$

where F_r is the radial component of dynamic bearing load. The load dependent friction factor f_1, for 62 series deep groove ball bearings is given by

$$f_1 = 0.0008\left(\frac{X_0 F}{C_0}\right)^{0.55} \qquad 9$$

and for 63 series deep groove ball bearings

$$f_1 = 0.0009\left(\frac{X_0 F}{C_0}\right)^{0.55} \qquad 10$$

Where C_0 is the static load rating of the bearing given by the manufacturer and X_0 is the radial factor, depending on the bearing design. X_0 = 0.6 for single row deep groove ball bearings. The total friction moment of each bearing M_{brg} may be obtained by adding the no-load moment M_0 and the load dependent moment M_1 giving

$$M_{brg} = M_0 + M_1 \qquad 11$$

The resistance force per idler roller acting due to the rolling element resistance of the bearings F_{brg} is then given by

$$F_{brg} = \frac{4M_{brg}}{D} \qquad (12)$$

Lip Seal Resistance

The outer lip seal forms the primary boundary between external contaminants entering the labyrinth seal, while the inner lip seal (if present) contains the lubricating grease within the bearing. Most lip seals used in idler rollers are made from nitrile rubber or similar compounds. The outer lip seals are typically fixed to the shaft and rub against the external surface of the labyrinth seal without any lubrication, while the design of the inner lip seal varies significantly between manufacturers. In order to approximate the resistance to rotation due to the lip seals, the following equation is derived from a graphical representation of the power loss for contact lip seals[16]. The force acting due to the resistance to rotation of the lip seal F_{ls}, is approximated by

$$F_{ls} = \frac{0.3\exp(25d_{ls})}{D\pi} \qquad (13)$$

where d_{ls} is the contact diameter of the lip seal. Equation 13 should only be considered an approximation due to the large variety of lip seal designs and configurations employed, in addition to the absence of any temperature correction factor, or allowance for dry or lubricated contact surfaces.

DESIGN CONSIDERATIONS

Based on the above equations, several observations can be made in relation to reducing rotating resistance. Figure 4 summarises the relationship between idler roller rotating resistance and temperature, demonstrating the contribution from each component in Figure 4(a) and, by way of example, measured data for different manufacturers in Figure 4(b). Lip seal friction and load dependent bearing friction are both considered independent of temperature, while the labyrinth seal and no-load bearing friction are dependent on internal shearing of the grease, and therefore dependent on grease viscosity and thus temperature. Decreasing rotating resistance with increasing temperature is also seen in Figure 2.

Figure 5 shows the relationship between idler roller rotating resistance, speed and load. Lip seal friction and load dependent bearing friction are both considered independent of rotational speed, while the labyrinth seal and no-load bearing friction are dependent on internal shearing of the grease, and therefore dependent on rotational speed. As the name implies, the load dependent bearing friction is the only friction component influenced by radial load, provided induced shaft deflections are not excessive.

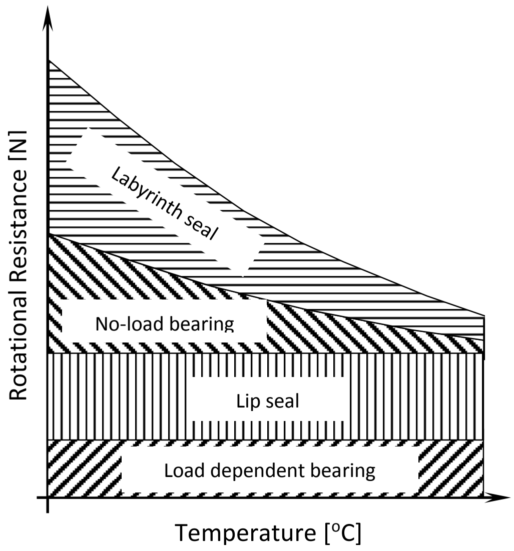

(a) Idler roller rotating resistance vs temperature

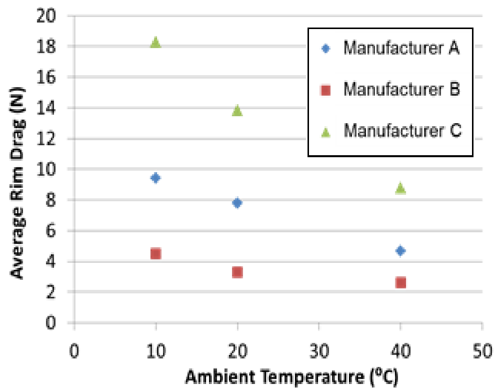

(b) Measured data

Figure 4. Idler roller rotating resistance versus temperature

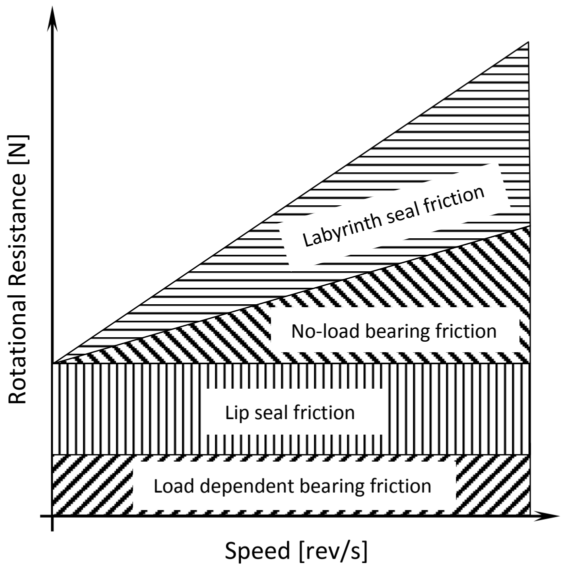

(a) Idler roller rotating resistance vs speed

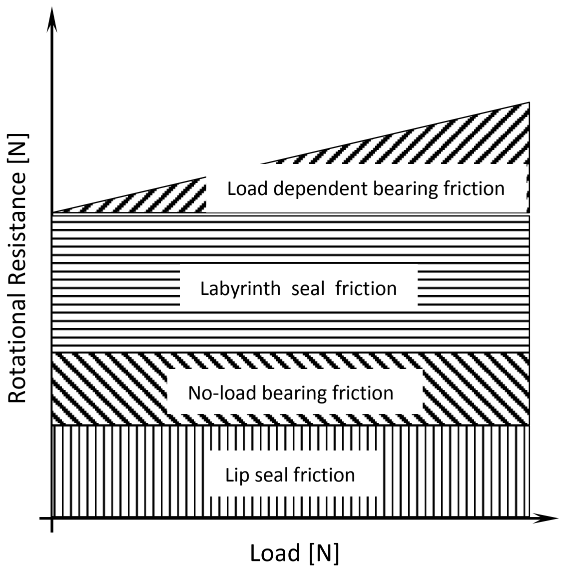

(b) Idler roller rotating resistance vs radial load

Figure 5. Idler roller rotating resistance versus speed and load

While standards provide a quality assurance measure and a means to compare one idler roller to another, acquired data is typically not directly applicable to conveyor design. It is evident from Figures 4 and 5 that from a design perspective, idler rollers should be tested as a function of ambient temperature (ranging between winter and summer conditions) at the required belt speed and load. If data matching the design parameters are not available, a knowledge of the trends captured in Figures 4 and 5 in conjunction with the preceding equations can provide an estimate. For example, if data for a single load (typically lower from SANS and DIN standard tests) are available, then the rotating resistance at higher loads can be extrapolated by calculating the additional load dependent bearing friction from Equation 8. Predicting variations with speed and temperature are more complex, given that the baseline friction due to lip seal friction and no-load bearing friction are unknown. As a minimum, idler roller rotating resistance data should be provided at the rotational speed, and for lower and upper operating temperatures.

The theoretical approximations discussed provide the fundamental theory to not only calculate the rotating resistance, but also to minimise the rotating resistance of the idler rollers at the design stage. Design considerations should include appropriate grease selection for the loading conditions and the temperature range in which the conveyor will be operating, in addition to efficient labyrinth seal design. While the calculated viscous drag of the labyrinth seal is only approximate due to the complicated velocity fields, the theoretical analysis proves instructive for labyrinth seal design. For example, labyrinth seals may be designed efficiently in order to prevent contaminant ingress, but at the same time reduce viscous drag by ensuring small gaps between stationary and rotating surfaces are employed closer to the shaft to reduce torque. Furthermore, gains can also be made by using larger diameter idler rollers to reduce rotational speed and therefore rotating resistance, in addition to the added advantage of increasing the fatigue life of bearings.

While the foregoing analysis has emphasised the benefits of reduced rotating resistance, the reliability of the idler roller is equally important, and careful consideration should also be given to the sealing effectiveness to prevent contamination and premature bearing failure.

4. CONVEYOR BELT INDENTATION, ROLLING RESISTANCE AND FLEXURE RESISTANCE

Indentation rolling resistance occurs due to the deformation of the pulley side cover of the conveyor belt as it is squeezed between the carcass and successive idler rollers. Belt flexure resistance occurs due to the vertical and transverse displacement of the belt between idler sets. Both resistances to movement of the belt are a result of internal energy losses within the conveyor belt that are absorbed by the belt as heat.

As the rubber belt travels over a conveyor idler roller, the pulley cover is indented by the weight of the belt and bulk material. The indentation cycle involves compression of the pulley cover as the belt drives into the roller, followed by recovery as the belt travels over the roller, as shown in Figure 6(a). Since the belt cannot recover at the same rate as it is compressed due to the viscoelastic (time dependent) properties of the rubber, an asymmetric pressure distribution forms, resulting in indentation rolling resistance. Figure 6(b) shows the resulting offset pressure distribution that leads to indentation rolling resistance.

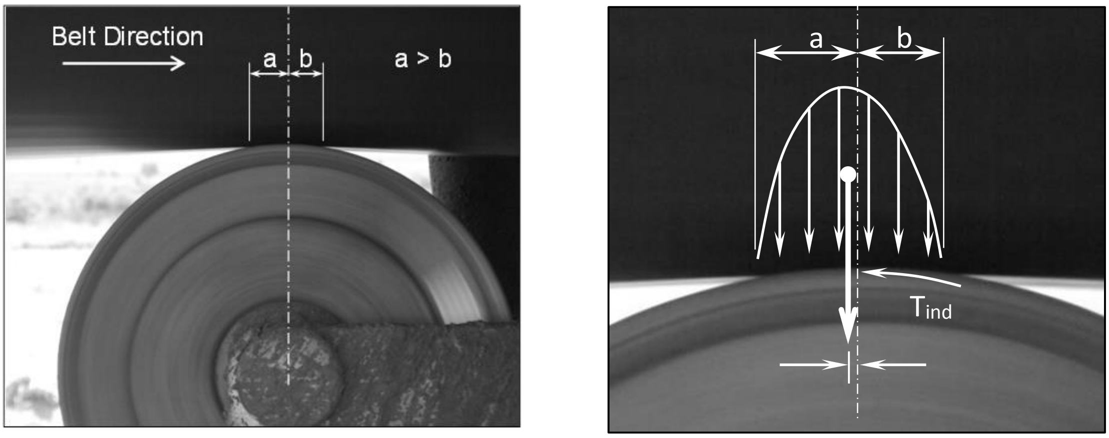

(a) Cyclic compression and recovery (b) Asymmetric pressure distribution

Figure 6. Indentation rolling resistance

The recovery time of a rubber cover is dependent on the viscoelastic properties of the rubber, and is therefore temperature, belt speed and strain dependent. Figure 7 shows typical relaxation modulus data for a pulley cover compound tested at varying strain levels.

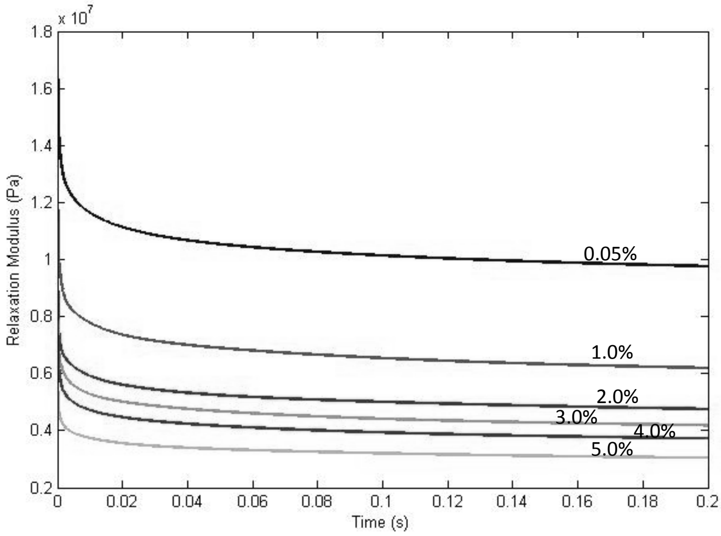

Figure 7. Relaxation modulus data for a pulley cover compound under varying strain

Flexure resistance of the conveyor belt occurs as a result of the cyclic transverse and longitudinal deflection of the belt between successive idler sets. Longitudinal deflection occurs due to belt sag, while transverse displacement occurs due to the opening and closing of the belt between idler sets. The resulting hysteresis losses in the carcass and carry and pulley covers lead to flexure resistance along the length of the conveyor.

CEMA[12] specifies two general approaches for determining indentation rolling resistance, namely the small sample and large sample methods. In both cases indentation rolling resistance is expressed as a function of normal load for a specific pulley cover compound, idler roller diameter, pulley cover thickness, temperature and belt speed.

SMALL SAMPLE METHOD

The small sample method uses a typical sample size of 3 mm x 12 mm x 30 mm from which the dynamic physical properties of the rubber are measured over a range of temperatures, strains and frequencies. These measurements utilise specialised Dynamic Mechanical Analysis (DMA) equipment and obtain the elastic storage modulus (E') and loss modulus (E") of the cover rubber sample. The measured dynamic properties are then used in a range of theoretical approaches to calculate the indentation rolling resistance as a function of normal load, and then based on an assumed loading distribution, used to calculate the indentation rolling resistance per idler set. Figure 8(a) shows the basis of a one-dimensional Winkler foundation using a generalised three-parameter Maxwell viscoelastic model, while Figure 8(b) shows a finite element approach. In the latter approach the forces acting on each element in the contact zone are calculated to determine the asymmetric pressure distribution acting on the idler roller via the belt.

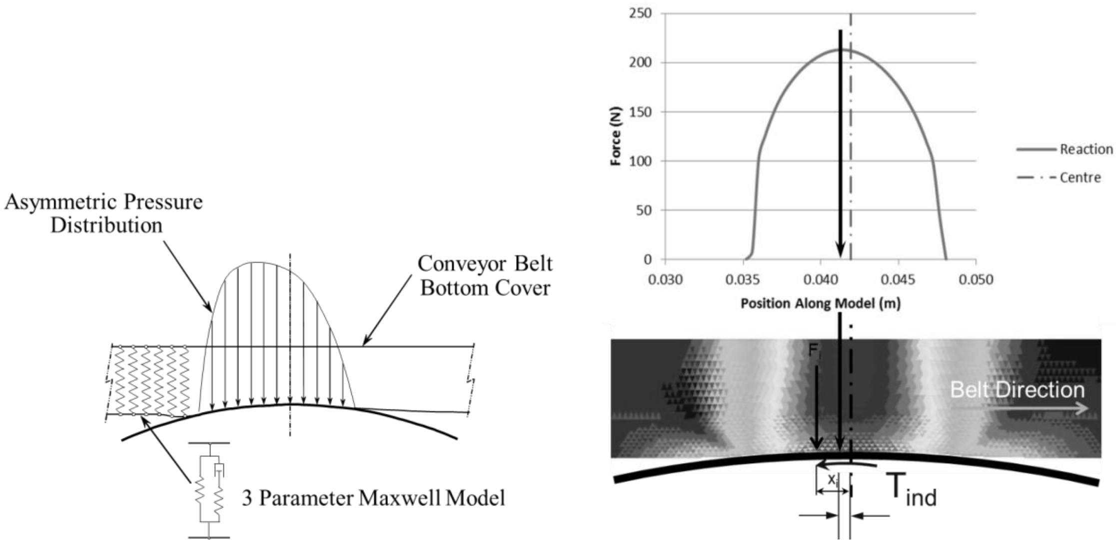

(a) Winker foundation model

(b) Finite element model
Munzenberger et al [17]

Figure 8. Indentation rolling resistance models

Accuracy of the small sample method relies heavily on the measurement of the dynamic rubber properties and the method of time-temperature superposition that is used to shift the measured data along the frequency axis. Models are often 'tuned' based upon extensive laboratory and/or field data to reach the levels of accuracy required for design purposes.

LARGE SAMPLE METHOD

The large sample method uses a full sample of belt, including the carcass and carry and pulley covers, with specified measurement facilities shown in Figure 9. Belts are approximately 400 mm to 600 mm wide, and either 4 800 mm or 29 000 mm long (spliced endless length), depending on the machine. The facility shown in Figure 9(b) provides the ability to measure both indentation rolling resistance and conveyor belt flexure resistance. Belt flexure is induced into the sample due to the deformation of the belt by the hold down rollers, with the position of the hold down determined by the belt sag ratio.

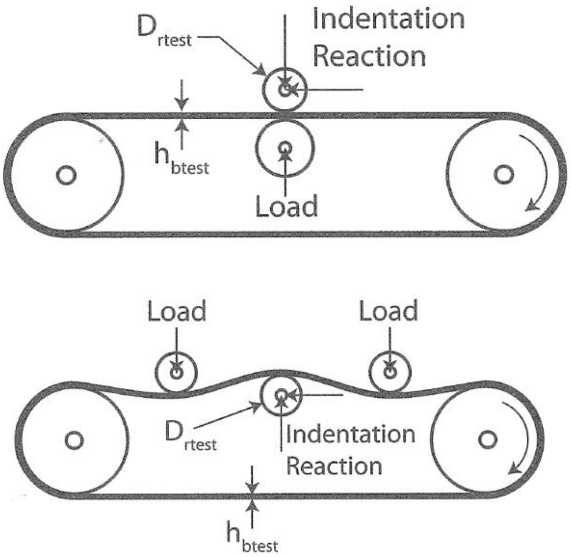

(a) DIN22123 large sample test method (b) Alternate large sample test method

Figure 9. CEMA's indentation rolling resistance large sample methods

CEMA[12]

Typical data from the large sample test method detailed in Figure 9(b) is illustrated in Figure 10. Indentation rolling resistance versus normal load data is given for a particular pulley cover rubber, idler roller diameter, cover thickness, temperature and belt speed for a range of belt sag ratios.

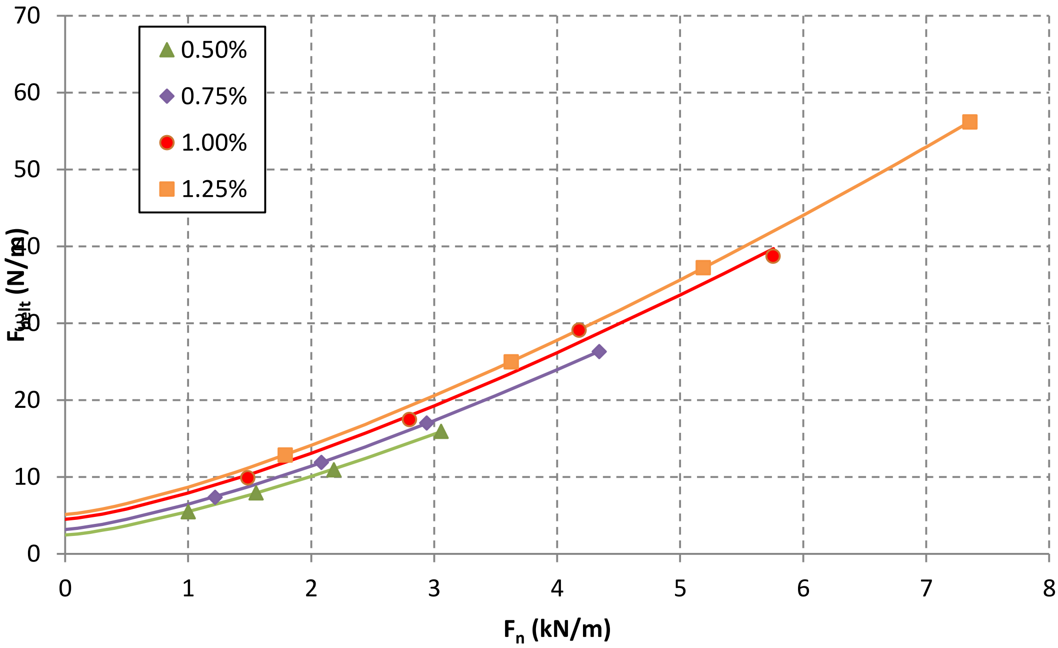

Figure 10. Indentation rolling resistance and belt flexure resistance versus normal load for a range of belt sag ratios (idler roller dia. = 150 mm, temperature = 40°C and beltspeed = 4 m/s)

In order to differentiate between the belt flexure and indentation rolling resistance components a least squares curve fit of Equation 14 is performed

$$F_{belt} = A + B.{F_n}^c \tag{14}$$

Where A is the y-intercept, B is the multiplier, F_n is the normal force applied to the belt and c is the exponent, where typically c = 4/3.

If tests were conducted without flexing the belt over the measurement idler roller the drag would be purely due to indentation rolling resistance and the experimental data would pass through the origin. The y-intercept is therefore assumed to be attributed to belt flexure resistance resulting in the relationship

$$F_{belt} = F_{b,flex} + F_{ind} \tag{15}$$

Where

$$F_{b,flex} = A \tag{16}$$

And

$$F_{ind} = B.{F_n}^c \tag{17}$$

NORMAL FORCE DISTRIBUTION

Conveyor belt flexure resistance and indentation rolling resistance are typically measured for a particular belt construction and pulley cover rubber as a function of normal load. To calculate the indentation rolling resistance per idler set it is important to accurately predict the load distribution across the idler set due to the belt and bulk material. CEMA[12] uses an average pressure distribution between the belt and idler roller based on an equivalent load distribution, while DIN22123[13] considers a normalised force distribution, incorporating a constant force distribution for the centre roller and an increasing linear distribution for the side rollers.

For the purpose of this paper the normal force components acting due to the belt and bulk material are shown schematically in Figure 11. From these forces, the force distribution along the length of the centre and side idler rollers is derived.

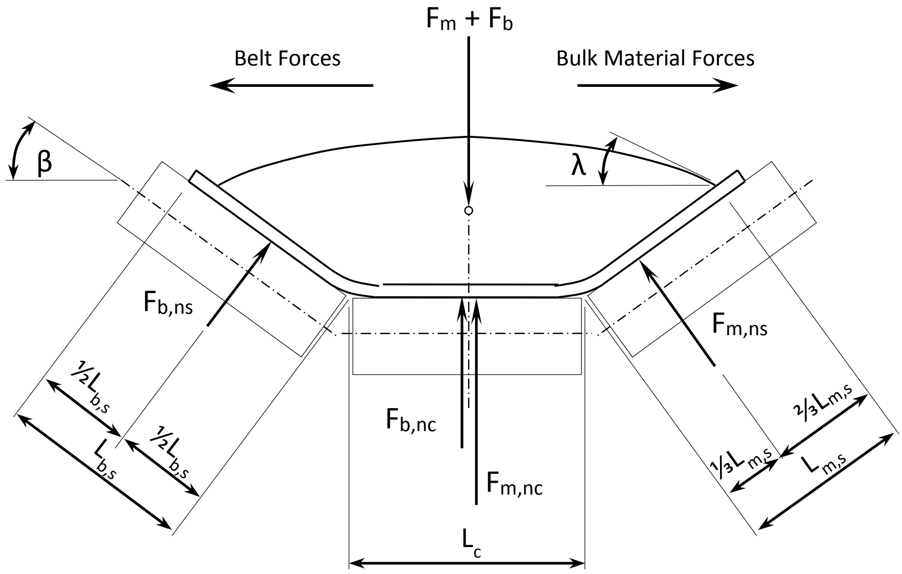

Figure 11. Normal forces acting on side and centre rollers due to the belt and bulk material

When considering the force distribution across the idler set due to the bulk material it is important to consider the increased loading on the side rollers caused by opening and closing the belt between successive idler sets. The opening and closing occurs following the vertical deflection of the belt. Work in this area was first undertaken by Krause and Hettler[18] who provided an analysis of the total force acting on the idler rollers as a result of the formation of active and passive stress states within the cross-section of the bulk material. The active pressure factor for opening the conveyor belt K_a, is expressed as

$$K_a = \left[\frac{\sin(\beta + \phi_i)/\sin\beta}{\sqrt{\sin(\beta - \phi_w)} + \sqrt{\dfrac{\sin(\phi_i + \phi_w)\sin(\phi_i - \lambda)}{\sin(\beta + \lambda)}}} \right]^2 \qquad 18$$

Where ϕ_w is the friction angle between the bulk material and the conveyor belt, ϕ_i is the internal angle of friction of the bulk material, β is the troughing angle and λ is the conveyor surcharge angle. The passive pressure factor for closing the conveyor belt K_p, is given by

$$K_p = \left[\frac{\sin(\beta - \phi_i)/\sin\beta}{\sqrt{\sin(\beta + \phi_w)} - \sqrt{\dfrac{\sin(\phi_i + \phi_w)\sin(\phi_i + \lambda)}{\sin(\beta + \lambda)}}} \right]^2 \qquad 19$$

Ilic[19] found through a series of laboratory and field experiments that the passive stress state, is in most cases, was not fully developed in the bulk material during closing. This is primarily due to the relatively small angle of transverse – opening and closing – belt deflection. On the basis of these findings, a reduction factor, R was applied to the passive pressure factor, K_p for the closing of the conveyor belt. The factor is dependent on the internal angle of friction of the bulk solid. For free flowing to moderate-to-handle bulk materials with internal angles of friction up to 45°, a value of 0.4 was found to be suitable, while for bulk materials with an internal angle of friction over 45°, a value of 0.2 was selected. The normal force, $F_{m,ns}$ acting on the inclined side of the belt (side idler rollers) due to the bulk material is therefore

$$F_{m,ns} = \frac{1}{4} a\rho g L_{m,s}^2 \left(K_a + RK_p\right)\cos\phi_w \tag{20}$$

Where a is the idler spacing, ρ is bulk density, $L_{m,s}$ is the length of bulk material in contact with the inclined side of the conveyor belt, and the active and passive stress states are assumed to act over half the idler spacing.

The normal force, $F_{m,nc}$ on the centre idler roller due to the bulk material is equal to the total load of the bulk material acting over the length of the idler spacing, less the vertical components of force exerted on the side rollers.

$$F_{m,nc} = a\rho g A - \frac{1}{2} a\rho g L_{m,s}^2 \left[K_a \cos(\beta - \phi_w) + RK_p \cos(\beta - \phi_w)\right] \tag{21}$$

Where A is the cross sectional area of bulk solids on the conveyor belt.

In addition to the normal forces generated by the bulk material, the normal forces caused by the weight of the belt must also be considered. The normal force $F_{b,ns}$ acting on the side idler roller due to the weight of the belt is

$$F_{b,ns} = \frac{L_{b,s}}{B_w} a q_b g \cos\beta \tag{22}$$

Where $L_{b,s}$ is the length of belt in contact with the side idler roller, B_w is the belt width and q_b is the mass of the belt per unit length. The normal force, $F_{b,nc}$ acting on the centre roll on account of the weight of the belt is

$$F_{b,nc} = \frac{L_c}{B_w} a q_b g \tag{23}$$

Figure 11 shows a typical normal force distribution acting across a three-roller idler set and the resulting indentation rolling resistance. As noted in DIN2123[13], the normal force distribution can be expressed as

$$F_n = \int_0^L q(z).\,dz \tag{24}$$

Where L is the total contact length of the bulk material with the belt and is given by

$$L = L_c + 2L_{m,s} \tag{25}$$

Where L_c is the contact length for the centre roller and $L_{m,s}$ for the side rollers.

The indentation rolling resistance along each idler roller is then derived from Equation 17 and is given by

$$F_{ind} = \int_0^L B.q(z)^c.dz \qquad 26$$

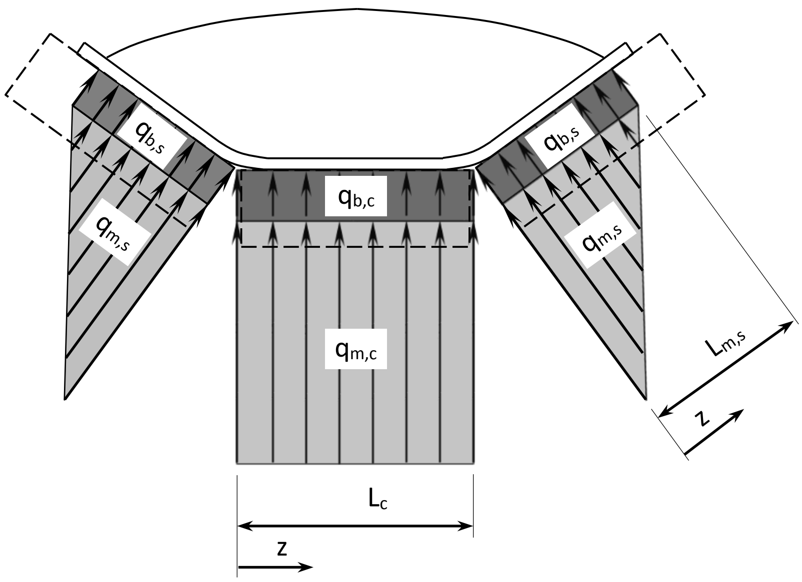

(a) Cross section showing normal force between idler rollers and belt

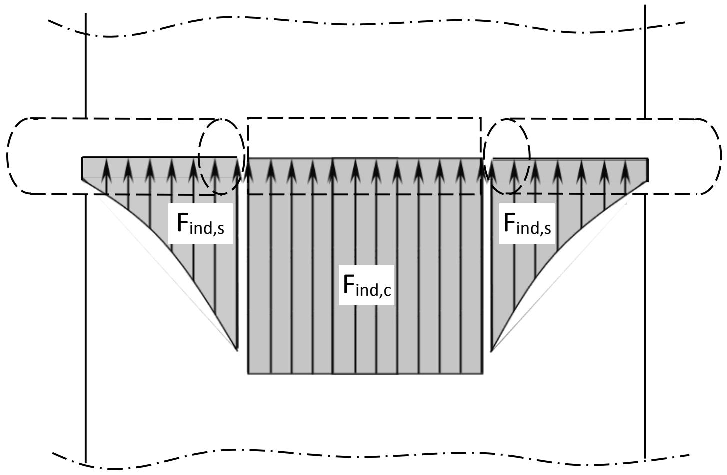

(b) Bottom view showing indentation rolling resistance distribution

Figure 12. Normal force distribution and resulting indentation rolling resistance for a three-roller troughing idler set

Figure 12 shows that the force distribution along the length of the centre roller is constant and is a sum of the force due to the belt $q_{b,c}(z)$ and bulk material $q_{m,c}(z)$.

Where

$$q_{b,c}(z) = \frac{F_{b,nc}}{L_c} \qquad 27$$

And

$$q_{m,c}(z) = \frac{F_{m,nc}}{L_c} \qquad 28$$

From Equation 26, the indention rolling resistance force acting on the centre roll is therefore given by

$$F_{ind,c} = \int_0^{L_c} B\left[q_{m,c}(z) + q_{b,c}(z)\right]^c . dz$$

$$F_{ind,c} = BL_c{}^{1-c}\left(F_{m,nc} + F_{b,nc}\right)^c \qquad 29$$

The force distribution along the side idler rollers is a combination of the force as a result of the belt $q_{b,s}(z)$ and a linearly decreasing load due to the bulk material $q_{m,s}(z)$.

Where

$$q_{b,s}(z) = \frac{F_{b,ns}}{L_{m,s}} \qquad 30$$

Bearing in mind that the force due to the belt weight is assumed to act over the length of contact of the bulk material rather than the belt contact length to simplify the load distribution.

The linearly decreasing force due to the bulk material is given by

$$q_{m,s}(z) = \frac{2F_{m,ns}}{L_{m,s}^2}\left(L_{m,s} - z\right) \qquad 31$$

Therefore

$$F_{ind,s} = \int_0^{L_c} B\left[q_{m,s}(z) + q_{b,s}(z)\right]^c . dz$$

$$F_{ind,s} = \frac{BL_{m,s}{}^{(1-c)}}{2F_{m,ns}(c+1)}\left[\left(2F_{m,ns} + F_{b,ns}\right)^{c+1} - F_{b,ns}{}^{c+1}\right] \qquad 32$$

The total indentation rolling resistance per idler set is therefore

$$F_{ind} = F_{ind,c} + 2.F_{ind,s} \qquad 33$$

$$F_{ind} = B\left(\frac{F_{m,nc}+F_{b,nc}}{L_c}\right)^c L_c + \frac{BL_{m,s}{}^{(1-c)}}{F_{m,ns}(c+1)}\left[\left(2F_{m,ns} + F_{b,ns}\right)^{c+1} - F_{b,ns}{}^{c+1}\right] \qquad 34$$

Where the normal forces are dependent on the belt, idler roller geometry and bulk material properties, the constants *B* and *c* are dependent on the measured indentation rolling resistance properties of the belt.

DESIGN CONSIDERATIONS

The preceding section provided methods to calculate the indentation rolling resistance and belt flexure resistance per idler roller set in terms of load, temperature, idler roller geometry, and bulk material and belt properties. These components were calculated using measured indentation rolling resistance and belt flexure data.

Indentation rolling resistance is dependent on the pulley cover rubber, normal load, temperature, idler roller diameter, cover thickness and belt speed. Indentation rolling resistance is considered independent of belt tension, and therefore belt sag, and is considered to be constant for each idler set along the length of the system. If horizontal and/or vertical curves are present, indentation rolling resistance varies according to the changing load profile.

The energy lost as a consequence of the flexure of the conveyor belt over each idler roller is dependent on the belt construction, temperature, and the extent of flexure which is dependent on the belt tension and longitudinal stiffness. Belt flexure resistance is typically small relative to indentation rolling resistance, although lighter loads and low temperatures can lead to belt flexure being significant. Belt flexure varies along the length of the conveyor due to changes in belt tension, however as this is a relatively small contribution, it can typically be considered constant.

Based on the preceding analysis it is evident the conveyor designer has many options during the design stage to reduce belt flexure and indentation rolling resistance. Some of the more common methods are discussed below.

Low Rolling Resistance Pulley Cover Compounds

Low rolling resistance pulley cover compounds are designed to maximise the energy restored during the recovery cycle. Significant energy savings can be made with the correct selection of pulley cover compound, however several factors should be taken into consideration. When evaluating the use of low rolling resistance compounds it is advisable to analyse potential energy savings over the range of average monthly temperatures as compounds are often temperature dependent[21]; furthermore, compounds that are temperature dependent will also be velocity dependent, and should be tested at the corresponding belt speed. To maximise the benefit of low rolling resistance compounds belt turnovers are typically employed on long belt conveyors to gain advantages on the return side.

Large Diameter Idler Rollers

Large diameter idler rollers have the advantage of reducing the contact stresses at the pulley cover and roller interface, therefore reducing indentation rolling resistance. For the same bearing and seal arrangement, larger idler rollers offer lower rotating resistance as a result of their larger radius. The larger radius also lowers the angular velocity which results in lower viscous resistance from the grease in the bearings and labyrinth seals and further reduces drag. In some cases it has proven more advantageous to utilise larger diameter idler rollers only for the more heavily loaded centre roller (see Figure 12(a)). Selectively using larger diameter rollers reduces investment cost and limits rotational mass.

Reduced Vertical Load

Reducing the vertical load on the belt reduces indentation rolling resistance. If for example, the load is halved, then from Equation 17 indentation rolling resistance will decrease by 2^c (i.e. 2 to the power of c, where typically c = 4/3) and result in a disproportionate decrease with load[7]. Clearly, any reduction in load requires an increase in belt speed to maintain a constant carrying capacity, which in turn, increases indentation rolling resistance, but at a lower rate.

Increased Idler Spacing

Reducing the number of times a belt is deflected between idler roller sets over the length of a system reduces the total conveyor belt flexure resistance. While this provides energy savings, they are relatively small in comparison to other components, with the most significant benefits of increased idler spacing resulting from reduced bulk material flexure resistance that is discussed Section 5.

Belt Carcass

It has been shown experimentally[7] that fabric reinforced belts exhibit greater indentation rolling resistance than steel cord belts, while steel cord belts with smaller diameter cables exhibit lower indentation rolling resistance than those with large diameter cables. These results prove the belt carcass plays an important role in indentation rolling resistance, and that any model or test should consider the elements and construction of the carcass. Furthermore, the belt carcass significantly influences the longitudinal stiffness of the belt and therefore the belt flexure resistance.

5. BULK MATERIAL FLEXURE RESISTANCE

Bulk material flexure resistance occurs due to the longitudinal and transverse displacement of the belt and bulk material between successive idler sets and the associated internal friction losses within the bulk material. As mentioned earlier, the belt and bulk material undergo complex interactions as the belt opens and closes transversely and is displaced vertically due to belt sag. The losses associated with the flexure resistance of the bulk material cannot easily be isolated and measured independently of the belt, therefore making this component of the main resistance the most difficult to quantify and accurately predict.

Several researchers have investigated the topic of bulk material flexure resistance. Investigations included analytical approaches[1,12,20], experimental investigations[22], and others have provided combined experimental and numerical methods[6,19]. For simplicity the approach outlined follows the theoretical approach of Spaans[1]. This approach considers the active and passive stress states that the bulk material undergoes as it travels from one idler set to the next. Spaans[1] notes that the bulk material flexure resistance is dominated by the longitudinal deflection, rather than the transverse deflection of the belt. He derives the longitudinal bulk material flexure $F_{m,flex}$, as

$$F_{m,flex} = \frac{F_m(F_b+F_m)}{\sqrt{T.EI}}\left(\frac{4.\sin\emptyset_i}{\cos^2\emptyset_i}\right)\frac{h^2}{12.a}e^{-\omega x} \qquad 35$$

Where EI is the flexural rigidity of the conveyor belt, T is the belt tension, $\emptyset_i$ is the internal angle of friction, h is the average height of bulk material above the centre idler roller, a is the idler spacing, $\omega = \sqrt{T/EI}$ and x is the distance from the idler roller set where the stiff trough-shaped belt transitions into a slack one and where the radius of curvature is smallest. Values of x typically are in the range 0.010 m < x < 0.040 m and are greater with increasing troughing angle, wider belts, greater tension and a stiffer belt carcass.

The relationship derived by Spaans[1] provides an estimate based on measured bulk material and belt properties, rather than relying on empirical approximations. Furthermore, the relationships resulting from Equation 35 correspond to the more complex numerical solutions and experimental findings[6,19].

DESIGN CONSIDERATIONS

From Equation 35 it is evident that the bulk material flexure resistance is heavily dependent on the geometry of the cross-section of bulk material with the flexure resistance increased by the height of bulk material squared. Furthermore, the flexure resistance of the bulk material decreases by the root of the belt tension, meaning less sag results in less belt and bulk material deflection and therefore less resistance.

To consider the coefficient of bulk material flexure resistance, $f_{m,flex}$, Equation 35 is divided by the sum of the weight of bulk material and belt to give

$$f_{m,flex} = \frac{F_m}{\sqrt{T.EI}} \left(\frac{4.\sin \emptyset_i}{\cos^2 \emptyset_i} \right) \frac{h^2}{12.a} e^{-\omega x} \qquad 36$$

To analyse the influence of bulk material internal friction and idler spacing, Figure 13(a) shows results from Equation 36 for a 1.2 m wide belt with a sag ratio of 1% conveying material with a bulk density of 1 000 kg/m^3. Several trends are immediately evident, including an increase in the bulk material flexure resistance coefficient with internal angle of friction, and a decrease with increasing idler spacing. In terms of the latter, bulk material flexure resistance per idler set increases with increasing idler roller spacing due to more work being done. However, the work per unit length decreases, resulting in an overall decrease in the bulk material flexure resistance coefficient with increasing idler spacing. In addition, other research[9] has shown the investment cost is typically reduced, since while belting costs increase (due to greater belt strengths), the increased cost is offset by a greater reduction in cost thanks to fewer idler sets.

Figure 13(b) shows the bulk material flexure resistance coefficient versus sag ratio for a 1.2 m wide belt, a bulk material density of 1 000 kg/m^3 and an internal angle of friction of 35^o. As expected, the bulk material flexure resistance coefficient increases with increasing belt sag ratio due to greater work from the increased vertical displacement of the bulk material.

In general, wider carry side idler roller spacing and higher belt tensions reduce bulk material flexure resistance, while bulk materials with greater internal friction generate more bulk material flexure. Likewise, wider idler roller spacing has the added advantage of less rollers and frames, usually with a resulting decrease in investment cost.

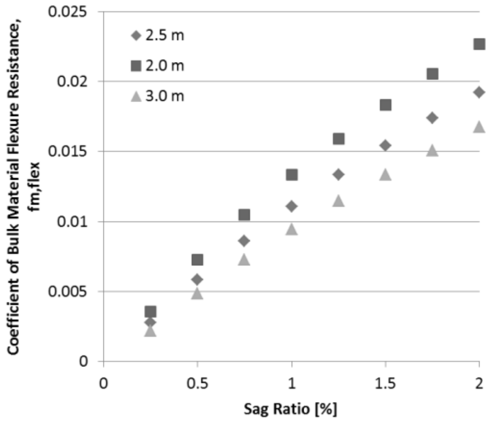

(a) Sag ratio = 1%

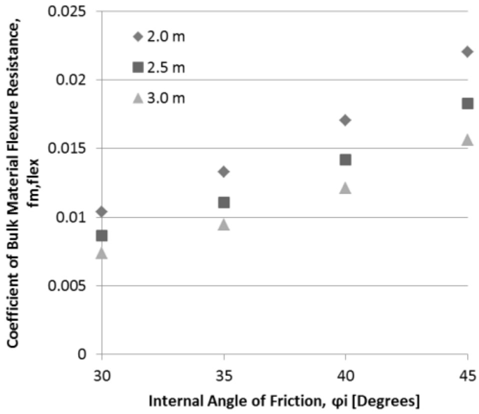

(b) Internal angle of friction = 35°

Figure 13. Coefficient of bulk material flexure resistance versus internal angle of friction and sag ratio (belt width = 1.2 m, bulk density = 1 000 kg/m^3)

6. CONCLUSION

This paper has presented a combination of theoretical models and measured data to assist in the design of energy efficient belt conveyors. A number of theoretical models to predict the main resistances of belt conveyors have been discussed with reference to testing standards and handbook methods. Through a comprehensive analysis of the motion resistances, key design parameters for energy efficient conveyor design were identified, enabling designers to select a combination of parameters that result in cost effective energy efficient solutions.

REFERENCES

1 Spaans, C.: The Calculation of the Main Resistance of Belt Conveyors; Bulk Solids Handling Vol. 11 (1991) No.4, pp.809-826.

2 Nordell, L.: The Channar 20 km Overland; A Flagship of Modern Belt Conveyor Technology; Bulk Solids Handling Vol. 11 (1991) No.4, pp.781-792.

3 Gladysiewicz, L., Krol, R. and Bukowski, J.: Tests of Belt Conveyor Resistance to Motion; Maintenance and Reliability Vol.3 (2011) pp.17-25.

4 Antoniak, J.: Resistances to the Motion in Mining Belt Conveyors Vol.6 (2001) No.2, pp.150-157.

5 Hager, M. and Geesmann, F.: Investigation of the Resistance to Motion of Belt Conveyors with a Large Mass Flow; Heavy Equipment Vol.54 (2002), No.3, pp.208-224.

6 Wheeler, C.: Analysis of the Main Resistances of Belt Conveyors, PhD Thesis, The University of Newcastle, 2003.

7 Hager, M. and Hintz, A.: The Energy Saving-Design of Belts for Long Conveyor Systems; Bulk Solids Handling Vol. 13 (1993) No.4 pp.749-758.

8 Greune, A. and Hager, M.: The Energy-Saving Design of Belt Conveyors; Bulk Solids Handling Vol. 10 (1990) No.3, pp.245-250.

9 Grimmer, K. and Kessler, F.: Considerations for Reducing Belt Conveyor Investment Costs; Bulk Solids Handling Vol. 17 (1997) No.1, pp.41-45.

10 DIN22101 Continuous Conveyors – Belt Conveyors for Loose Bulk Materials – Basis for Calculation and Dimensioning, 2000.

11 ISO5048:1989 Continuous Mechanical Handling Equipment – Belt Conveyors with Carry Idlers – Calculation of Operating Power and Tensile Forces, International Standard, Switzerland, 1989.

12 CEMA: Belt Conveyors for Bulk Materials, 7th Ed. 2014.

13 DIN 22123 Conveyor Belts - Indentation Rolling Resistances Of Conveyor Belts Related To Beltwidth - Requirements, Testing, 2012.

14 SANS1313-3 Conveyor Belt Idlers – Part 3 – Performance Specifications for Troughed Belt Conveyor Idlers for Idler Roller Rotational Speeds of up to 750 rpm, 2012.

15 Palmgren, A.: Ball and Roller Bearing Engineering, SKF Industries, Inc, Philadelphia, 1959.

16 SKF Web Site: skf.com

17 Munzenberger, P. and Wheeler, C.: Advances in Predicting the Indentation Rolling Resistance of Belt Conveyors, Beltcon 17, 2013.

18 Krause, F. and Hettler, W.: Die Belastung der Tragrollen von Gurtbandforderern mit dreiteiligen Tragrollenstationen infolge Fordergut unter Beachtung des Fordervorganges und der Schuttguteigenschaften; Wissenschaftliche Zeitschrift der Technischen Hochschule Otto von Guericke, Germany, 18 (1974), Heft 6/7.

19 Ilic, D.: Bulk Solid Interactions in Belt Conveying Systems, PhD Thesis, The University of Newcastle, 2013.

20 Mulani, I.: Engineering Science and Application Design for Belt Conveyors, 1st Ed., Saurabh Creation, India, 2001.

21 O'Shea, J., Wheeler, C., Munzenberger, P. and Ausling, G.: The Influence of Viscoelastic Property Measurements on the Predicted Rolling Resistance of Belt Conveyors, J. Appl. Polym. Sci. 2014, 131, 40755.

22 Limberg, H.: Untersuchung der Trumbezogenen Bewegungswidererstände von Gurtförderanlagen: Ph.D Thesis, University of Hannover, Germany, (1988).

ABOUT THE AUTHORS

CRAIG WHEELER

Dr Craig Wheeler is an associate professor in the School of Engineering at the University of Newcastle, Australia and associate director of TUNRA Bulk Solids. He worked as a mechanical engineer for BHP Billiton for eleven years and then as a research fellow at the Centre for Bulk Solids and Particulate Technologies for four years. He was appointed as an academic in the discipline of Mechanical Engineering in 2003.

A/Prof Craig Wheeler
Centre for Bulk Solids and Particulate Technologies
School of Engineering
The University of Newcastle
University Drive
Callaghan NSW 2308 AUSTRALIA
Telephone: (+61 2) 4033 9037
Email: Craig.Wheeler@newcastle.edu.au

PAUL MUNZENBERGER

Paul Munzenberger completed an apprenticeship as a fitter machinist in early 2001, and spent several years afterwards as a tradesman principally involved with maintenance and repair of 'Cable Belt' and conventional trough conveyors, as well as a variety of other equipment associated with coal handling and preparation. He completed his Bachelor's degree in Mechanical Engineering at the University of Newcastle in 2007 with first class honours. He is currently studying part time for a PhD in Mechanical Engineering in the field of belt conveying technology, while working as a research engineer for TUNRA Bulk Solids.

Paul Munzenberger
TUNRA Bulk Solids Research Associates
The University of Newcastle
University Drive
Callaghan NSW 2308 AUSTRALIA
Telephone: (+61 2) 403 39012
Email: Paul.Munzenberger@newcastle.edu.au

Daniel Ausling

Daniel Ausling is employed as a consulting engineer with TUNRA Bulk Solids. He holds a BE degree in Mechanical Engineering and is completing a PhD on a part time basis in the area of optimisation of long overland belt conveyor systems. He has experience in the belt conveying field, including design areas, belt testing and idler roller testing. He also has experience in the design of transfer chutes for materials handling operations and the application of continuum and DEM modelling of solids flow, and the use of these techniques in commercial design applications.

Daniel Ausling
TUNRA Bulk Solids Research Associates
The University of Newcastle
University Drive
Callaghan NSW 2308 AUSTRALIA
Telephone: (+61 2) 4033 9043
Email: Daniel.Ausling@newcastle.edu.au

Brendan Beh

Brendan Beh completed his Bachelor's degree in Mechanical Engineering at the University of Newcastle in 2008. Since 2008 he has worked as a research associate in the School of Engineering where he has been actively involved in projects focusing on conveyor belt testing and energy reduction. He is currently enrolled as a research master in the area of belt conveying technology in the School of Engineering while working part time for TUNRA Bulk Solids.

Brendan Beh
Centre for Bulk Solids and Particulate Technologies
School of Engineering
The University of Newcastle
University Drive
Callaghan NSW 2308 AUSTRALIA
Telephone: (+61 2) 4033 9032
Email: Brendan.Beh@newcastle.edu.au

.